THE ASTROPHYSICAL JOURNAL, 422:671–680, 1994 February 20

TIMING BEHAVIOR OF 96 RADIO PULSARS

Z. ARZOUMANIAN,[1] D. J. NICE,[2] AND J. H. TAYLOR[3]
Joseph Henry Laboratories and Department of Physics, Princeton University, Princeton, NJ 08544
AND
S. E. THORSETT[4]
Owens Valley Radio Observatory, California Institute of Technology, MS 105-24, Pasadena, CA 91125
Received 1993 June 1; accepted 1993 August 25

ABSTRACT

We present results from observations of 104 pulsars made between 1989 August and 1993 April, including timing solutions for 96 of them. Pulse profiles were recorded at four frequencies in the range 0.4–1.64 GHz, yielding topocentric pulse arrival times with uncertainties of order 10^{-3} periods. Models fitted to the timing data yield accurate positions, periods, period derivatives, and dispersion measures for each pulsar. Nine of the measured period derivatives are new, and most of the parameters represent improvements upon previous measurements. In a few cases we correct some erroneous parameter values from the published literature. A glitch was observed in the PSR B1800−21 pulse arrival times, and we fit a simple exponential model to the post-glitch recovery. We present graphs of the observed pulse shapes and their evolution with frequency, a table of measured pulse widths, and quantitative estimates of the long-term timing stability of each pulsar.

Subject heading: pulsars: general

1. INTRODUCTION

In anticipation of the launch of the *Compton Gamma Ray Observatory*, and mindful of the requirement for accurate, contemporaneous timing parameters in order to observe pulsars at gamma-ray energies, we began an extensive series of pulsar timing observations with the NRAO 43 m telescope in 1989 August. About 120 pulsars north of −45° declination were selected, with preference given to objects considered most likely to be detectable in gamma rays. Our observing list also included a number of pulsars with unmeasured period derivatives or poorly determined positions or dispersion measures. Fifteen pulsars were dropped from the program when they proved too weak to be observed with integration times of a few minutes, and for various reasons another eight objects on the list were observed only occasionally. The remaining 96 pulsars were observed in most or all of 14 observing sessions scheduled at approximately 3-month intervals since the project began. Phase-connected timing solutions have been obtained for all of these pulsars.

We describe the data acquisition system, observing procedure, and method of data analysis in § 2. In § 3 we present numerical results, including pulsar parameters, estimates of timing errors due to clock noise, and a description of a glitch in PSR B1800−21. In § 4 we present profiles of the pulsars. In § 5 we make some comparisons of our measured parameters with previous work, and we comment on a few results of particular interest.

2. OBSERVATIONS AND ANALYSIS

Observing sessions for this program were scheduled four times each year and generally lasted about 4 days. From 1989 August through 1990 February each observing session included observations at frequencies near 0.4 and 1.33 GHz. After that time, frequencies of 0.8, 1.33, and (occasionally) 1.64 GHz were used. A digital Fourier transform spectrometer analyzed the received signal into a large number of spectral channels and synchronously averaged the detected intensities into 128 phase bins spanning the topocentric pulsar period. During 1989 and 1990, 256 spectral channels in each of two orthogonal polarizations were used to cover a 20 MHz passband. In early 1991 the spectrometer hardware was doubled, and we subsequently used 2 × 512 channels covering 40 MHz. Individual pulsars were observed each day for four or five separate integrations each lasting 2–3 minutes.

All critical timing signals and reference frequencies required to operate the digital spectrometer were phase-locked to a local hydrogen maser frequency standard. A precomputed ephemeris was used to keep the hardware synchronized with the topocentric pulsar signal, accurately compensating for pulsar spin-down, the motion of the observatory, and the orbital motions of binary pulsars. The recorded data for a given observation consisted of a matrix of numbers representing average intensity as a function of frequency and pulse phase, along with such bookkeeping details as observing frequency and precise start times. Time offsets between the maser clock and UTC(NIST) were monitored with a Global Positioning System (GPS) receiver; clock uncertainties were kept below 1 μs, and could be safely ignored in subsequent processing.

Radio frequency interference was removed from the data matrices by an automated procedure which deleted spectral channels and time bins with anomalously large intensities. Differential delays caused by dispersion in the interstellar plasma were compensated by shifting the profiles for each frequency channel to a reference frequency at the midpoint of the passband. The necessary time shifts were calculated using the best available estimate of the pulsar's dispersion measure (DM). In a few cases our measured DM was sufficiently different from the assumed value to warrant a second iteration of this step, using the newly obtained value. After dispersion removal the

[1] E-mail: zaven@pulsar.princeton.edu.
[2] E-mail: david@pulsar.princeton.edu. Present address: NRAO, Edgemont Road, Charlottesville, VA 22903.
[3] E-mail: joe@pulsar.princeton.edu.
[4] E-mail: set@surya.caltech.edu.

TABLE 1

OBSERVED PARAMETERS OF 96 PULSARS[a]

PSR	R. A. (J2000)	±	Dec. (J2000)	±	DM ($cm^{-3}pc$)	±	P (s)	±	$\dot{P}$ (10^{-15})	±	Epoch (MJD)	σ_W (ms)	σ_R (ms)	Δ_8	Note
B0011+47	00:14:17.75	7	+47:46:34.4	7	31.1	2	1.24069897808	5	0.563	3	48416.0	5.17	5.17	<−1.3	
B0031−07	00:34:08.83	10	−07:21:51	3	11.3	11	0.94295105616	5	0.407	3	48382.0	6.81	6.81	<−1.2	
B0059+65	01:02:32.91	8	+65:37:13.3	5	65.84	13	1.67916356448	5	5.944	3	48382.0	2.94	2.95	<−1.5	
B0105+65	01:08:22.97	13	+66:08:31.3	10	30.2	2	1.2836580955	3	12.95	2	48464.0	3.59	24.94	0.0	
B0114+58	01:17:38.66	2	+59:14:38.4	2	49.45	5	0.1014383748286	11	5.84556	7	48382.0	0.59	0.96	−1.8	
B0136+57	01:39:19.770	3	+58:14:31.85	3	73.75	9	0.272449791574	5	10.7003	3	48382.0	0.21	2.34	−1.0	
B0144+59	01:47:44.665	5	+59:22:03.19	5	40.102	12	0.1963212513227	4	0.25699	2	48416.0	0.32	0.32	<−2.6	
B0154+61	01:57:50.00	7	+62:12:27.1	8	29.8	3	2.35172383222	13	188.841	9	48416.0	4.00	6.27	−0.9	
B0301+19	03:04:33.01	12	+19:32:56	6	15.73	6	1.387584344814	18	1.2959	11	48382.0	2.06	2.09	−1.8	
B0320+39	03:23:26.69	7	+39:44:52.5	18	25.4	9	3.03207190633	13	0.638	8	48382.0	5.61	5.61	<−1.3	
B0331+45	03:35:16.652	7	+45:55:53.41	15	47.155	20	0.2692005399801	10	0.00739	7	48416.0	0.58	0.59	−2.3	
B0353+52	03:57:44.815	4	+52:36:57.69	7	103.650	12	0.1970300350276	4	0.47666	3	48416.0	0.37	0.37	<−2.6	
B0355+54	03:58:53.707	3	+54:13:13.62	4	57.14	6	0.1563819489689	12	4.39747	7	48382.0	0.16	0.75	−1.4	
B0402+61	04:06:30.052	14	+61:38:40.76	16	65.22	3	0.594573579580	5	5.5863	4	48416.0	0.93	1.19	−1.6	
B0450+55	04:54:07.680	6	+55:43:41.73	9	14.602	18	0.340729130149	3	2.3656	2	48416.0	0.49	1.34	−1.2	
B0458+46	05:02:04.570	11	+46:54:06.1	3	42.09	4	0.638565320407	5	5.5831	3	48383.0	1.37	1.38	<−2.1	
B0523+11	05:25:56.445	4	+11:15:19.0	3	79.294	19	0.3544375952751	14	0.07362	8	48382.0	0.59	0.60	<−2.4	
B0540+23	05:43:09.66	2	+23:29:03	11	77.698	7	0.2459740892957	10	15.42378	6	48382.0	0.20	0.51	−1.8	
B0559−05	06:01:58.983	4	−05:27:50.53	12	80.514	19	0.3959690573556	15	1.30265	9	48382.0	0.62	0.62	<−2.4	
B0611+22	06:14:17.10		+22:29:58		96.89	8	0.33495352692	10	59.538	3	48422.0	0.82	44.41	0.2	†
B0626+24	06:29:05.742	17	+24:15:47	4	84.20	3	0.476622653938	3	1.99705	19	48382.0	0.44	0.73	<−2.5	
B0643+80	06:53:15.08	13	+80:52:00.8	5	33.27	15	1.21444043044	2	3.7977	18	48465.0	2.09	2.10	<−1.5	
B0656+14	06:59:48.103	17	+14:14:19.2	14	14.02	5	0.384885025950	7	55.0134	4	48423.0	1.90	2.49	−1.3	
B0727−18	07:29:32.355	11	−18:36:43.22	20	61.30	4	0.51015815294	4	18.976	2	48382.0	1.09	9.99	−0.4	
B0740−28	07:42:49.073		−28:22:44.02		73.75	2	0.166760919792	2	16.81152	18	48382.0	0.21	3.26	−1.0	†
B0751+32	07:54:40.73	5	+32:31:56.5	18	40.04	15	1.44234944724	3	1.0802	19	48383.0	2.74	2.74	<−1.5	
B0809+74	08:14:59.44	4	+74:29:05.79	14	4.8	10	1.292241435531	16	0.1683	8	48382.0	1.06	1.06	<−1.9	
B0818−41	08:20:15.45	7	−41:14:36.4	7	113.4	2	0.54544553611	2	0.0189	13	48383.0	6.26	6.26	<−1.4	
B0823+26	08:26:51.384	9	+26:37:22.4	3	19.458	15	0.530660797580	8	1.7094	4	48383.0	0.27	1.34	−1.2	
B0834+06	08:37:05.660	15	+06:10:15.0	6	12.87	4	1.273768080672	15	6.7995	7	48362.0	1.36	1.37	<−1.9	
B0906−17	09:08:38.175	6	−17:39:37.77	11	15.89	2	0.4016256029613	18	0.66959	10	48383.0	0.72	0.73	−2.1	
B0919+06	09:22:14.071	6	+06:38:25.6	3	27.13	13	0.430619672580	7	13.7202	5	48412.0	0.38	2.43	−1.2	
B0940+16	09:43:30.0	4	+16:31:34	16	20.0	3	1.08741772517	7	0.086	5	48500.0	7.16	7.19	<−1.0	*
B1039−19	10:41:36.21	2	−19:42:13.8	4	33.87	8	1.38636804563	2	0.9446	11	48383.0	2.18	2.23	−1.6	
B1112+50	11:15:38.37	4	+50:30:12.8	5	9.32	15	1.65643955514	5	2.493	2	48383.0	3.31	3.36	−1.5	
B1114−41	11:16:43.094	9	−41:22:44.64	12	40.53	3	0.943157882843	7	7.9536	4	48383.0	0.82	0.93	−1.8	
B1237+25	12:39:40.420	7	+24:53:49.55	17	9.22	4	1.382449256685	9	0.9605	5	48383.0	0.77	0.78	<−2.2	
B1322+83	13:21:46.0	3	+83:23:38.4	4	13.27	10	0.670037393641	18	0.5660	10	48383.0	2.41	2.42	<−1.5	
B1508+55	15:09:25.724	9	+55:31:33.01	8	19.63	3	0.739681265668	6	5.0078	3	48383.0	0.50	0.79	−1.6	
B1540−06	15:43:30.161	14	−06:20:45.2	6	18.48	5	0.709063990668	10	0.8834	5	48383.0	0.90	1.20	−1.7	
B1541+09	15:43:38.84	2	+09:29:16.1	7	35.16	7	0.748448403647	14	0.4327	9	48382.0	3.75	3.88	−1.3	
B1552−23	15:55:33.16	5	−23:41:11	3	51.97	6	0.532577650368	7	0.6922	4	48382.0	1.50	1.67	−1.6	
B1552−31	15:55:17.966	7	−31:34:19.6	3	73.066	15	0.518109771780	2	0.06218	12	48382.0	0.77	0.78	−2.3	*
B1604−00	16:07:12.094	4	−00:32:40.90	19	10.73	2	0.4218162718266	19	0.30610	11	48419.0	0.53	0.53	<−2.3	
B1620−09	16:23:17.70	3	−09:08:48.1	14	68.15	9	1.27644574527	3	2.5798	17	48382.0	2.05	2.07	<−1.7	
B1649−23	16:52:58.43	13	−24:04:03	16	68.31	14	1.70373903957	5	3.162	3	48382.0	3.37	3.39	<−1.6	*
B1700−32	17:03:22.540	14	−32:41:47.4	12	110.30	8	1.211785002035	19	0.6597	10	48381.0	2.14	2.15	<−1.8	
B1702−19	17:05:36.108	6	−19:06:38.5	7	22.920	14	0.2989872836669	10	4.13828	6	48331.0	0.39	0.40	−2.3	
B1706−16	17:09:26.458	7	−16:40:57.6	6	24.91	3	0.653054718982	7	6.3088	4	48367.0	0.42	0.73	−1.5	
B1717−29	17:20:34.13	2	−29:33:17	3	42.63	11	0.620448269870	15	0.7456	7	48381.0	2.43	2.43	<−1.6	
B1718−32	17:22:02.955	4	−32:07:44.9	3	126.035	19	0.4771574338858	18	0.64714	11	48381.0	0.45	0.49	−2.2	
B1719−37	17:22:59.17	4	−37:12:03.7	6	99.50	4	0.236173191636	4	10.8545	3	48381.0	0.36	2.08	−1.7	
B1730−22	17:33:26.42	6	−22:28:36	16	41.19	9	0.871682831914	17	0.0421	9	48417.0	2.04	2.04	<−1.7	*
B1732−07	17:35:04.972	3	−07:24:52.38	19	73.54	2	0.4193348081160	17	1.21496	9	48381.0	0.47	0.48	−2.3	*
B1738−08	17:41:22.54	3	−08:40:32.7	16	74.93	15	2.04308240001	6	2.274	4	48417.0	3.70	3.70	<−1.5	
B1742−30	17:45:56.299	2	−30:40:23.6	3	88.387	11	0.3674273631090	16	10.66487	10	48381.0	0.23	0.47	−1.8	
B1800−21	18:03:51.35		−21:37:07.2		233.9	3	0.1336076403	2	134.229	3	48700.0	0.93	1.09	−1.6	†
B1813−26	18:16:35.45	3	−26:49:58	4	128.03	12	0.592885128398	14	0.0665	7	48382.0	2.70	2.70	<−1.7	*
B1819−22	18:22:58.97	15	−22:56:49	54	121.14	15	1.87426847638	5	1.353	3	48382.0	3.19	3.20	<−1.6	*
B1820−31	18:23:46.783	2	−31:06:49.74	20	50.253	13	0.284053912446	3	2.92294	18	48382.0	0.24	1.35	−1.3	
B1822−09	18:25:30.596	6	−09:35:22.8	4	19.46	4	0.768979397911	12	52.3636	7	48381.0	0.86	1.75	−1.2	
B1829−08	18:32:37.014	9	−08:27:03.4	5	300.81	10	0.647287745864	7	63.8877	6	48541.0	1.08	1.08	<−1.7	
B1834−06	18:37:14.88	18	−06:53:02	7	316.1	16	1.9058086507	4	0.72	5	48650.0	15.31	15.37	<−0.2	
B1839+56	18:40:44.59	5	+56:40:55.6	4	26.54	17	1.65286180946	5	1.495	3	48381.0	3.12	3.15	<−1.5	
B1857−26	19:00:47.578	11	−26:00:43.8	11	38.06	3	0.612209195437	3	0.20419	16	48381.0	0.66	0.66	<−2.3	

TABLE 1—*Continued*

PSR	R. A. (J2000)	±	Dec. (J2000)	±	DM ($cm^{-3}pc$)	±	P (s)	±	$\dot{P}$ (10^{-15})	±	Epoch (MJD)	σ_W (ms)	σ_R (ms)	Δ_8	Note
B1859+03	19:01:31.783	4	+03:31:06.25	10	401.25	2	0.65544923094	3	7.481	2	48464.0	0.30	4.70	−0.6	
B1859+07	19:01:38.951	15	+07:16:34.7	4	252.81	16	0.643998410916	13	2.3375	13	48591.0	1.86	1.92	−1.1	
B1907+10	19:09:48.695	3	+11:02:03.29	7	149.9	3	0.283640003888	4	2.6361	2	48382.0	0.36	1.63	−1.7	
B1914+09	19:16:32.337	5	+09:51:26.10	12	60.92	5	0.2702541068864	14	2.51844	7	48381.0	0.66	0.68	−2.1	
B1914+13	19:16:58.699	8	+13:12:49.7	3	236.858	18	0.281842034269	5	3.6559	3	48382.0	0.43	2.06	−1.5	
B1915+13	19:17:39.784	2	+13:53:57.06	9	94.494	8	0.1946301238710	9	7.19809	6	48382.0	0.15	0.55	−2.9	
B1919+21	19:21:44.820	9	+21:53:02.54	16	12.45	4	1.337302088331	15	1.3477	7	48382.0	0.92	0.94	−2.1	
B1929+10	19:32:13.900	2	+10:59:31.99	7	3.13	3	0.226517820862	2	1.15661	12	48381.0	0.11	0.84	−1.5	
B1929+20	19:32:08.030	3	+20:20:46.30	6	211.007	17	0.268216854361	3	4.21630	18	48381.0	0.34	1.14	−1.5	
B1930+22	19:32:22.68	4	+22:20:56.6	12	219.05	4	0.144455311469	16	57.5318	9	48382.0	0.94	13.07	−0.3	
B1935+25	19:37:01.268	5	+25:44:13.73	7	53.24	3	0.2009801308966	8	0.64289	5	48415.0	0.63	0.63	<−2.3	*
B1937−26	19:41:00.411	8	−26:02:05.9	5	50.039	19	0.4028577689443	14	0.95604	7	48382.0	0.39	0.40	<−2.5	
B1943−29	19:46:51.72	3	−29:13:46.7	15	44.19	11	0.959447886144	19	1.4885	9	48383.0	1.67	1.74	−1.7	
B1944+17	19:46:53.053	9	+18:05:41.33	19	16.11	5	0.440618476059	4	0.0244	2	48381.0	1.37	1.37	<−1.9	
B1952+29	19:54:22.557	9	+29:23:17.23	14	8.05	6	0.426676786488	3	0.00164	19	48415.0	0.99	0.99	<−2.0	
B2000+32	20:02:04.40	3	+32:17:18.1	3	142.03	13	0.69675085073	14	105.206	8	48381.0	2.80	19.33	−0.1	
B2002+31	20:04:52.292	12	+31:37:09.95	17	234.72	5	2.11125608290	2	74.5411	14	48380.0	1.39	1.44	−1.7	
B2003−08	20:06:16.31	5	−08:07:02	2	32.1	3	0.58087133152	3	0.0452	15	48383.0	4.74	4.80	<−1.4	
B2021+51	20:22:49.867	6	+51:54:50.31	5	22.5	5	0.529197379220	2	3.06554	11	48382.0	0.43	0.46	−2.0	
B2022+50	20:23:41.942	5	+50:37:34.81	4	32.97	3	0.3726187682316	11	2.51198	11	48591.0	0.37	0.37	<−2.2	
B2106+44	21:08:20.478	10	+44:41:48.79	10	139.88	3	0.414870534238	3	0.08619	15	48382.0	1.14	1.14	<−2.1	
B2111+46	21:13:24.295	14	+46:44:08.68	11	141.9	5	1.014684902209	12	0.7115	6	48382.0	1.03	1.08	−1.7	
B2148+52	21:50:37.742	7	+52:47:49.67	5	148.94	2	0.3322045268581	13	10.10608	8	48382.0	0.64	0.65	<−2.5	
B2154+40	21:57:01.821	13	+40:17:45.88	14	70.61	6	1.525265368687	17	3.4257	9	48382.0	1.46	1.46	<−2.0	
B2217+47	22:19:48.136	4	+47:54:53.83	4	43.516	17	0.5384692479485	19	2.76503	9	48382.0	0.31	0.31	<−2.5	
B2224+65	22:25:52.36	2	+65:35:33.78	12	36.16	5	0.682537459727	5	9.6552	3	48382.0	1.31	1.33	−2.0	
B2255+58	22:57:57.711	4	+59:09:14.95	3	151.071	12	0.368245626351	3	5.75370	16	48419.0	0.31	1.04	−1.5	
B2319+60	23:21:55.19	4	+60:24:30.7	3	94.78	11	2.25648786737	4	7.037	2	48383.0	2.84	2.85	<−1.7	
B2324+60	23:26:58.704	5	+61:13:36.50	3	122.688	19	0.2336519310508	5	0.35263	3	48416.0	0.36	0.36	<−2.6	*
B2334+61	23:37:05.80	4	+61:51:01.6	2	58.38	9	0.49527878465	3	191.8103	19	48419.0	2.03	8.13	−0.6	
B2351+61	23:54:04.710	17	+61:55:46.78	12	94.34	6	0.944782448983	9	16.2641	4	48382.0	0.82	0.84	−2.0	

[a] Uncertainties refer to the least significant digits quoted.
* Pulsars with newly measured period derivatives.
† Pulsars for which a published interferometric position was held fixed in the fit for spin parameters.

single-channel profiles of both polarizations were summed to form a total-intensity mean profile for each integration.

A pulse time of arrival (TOA) was obtained for each integration by projecting the observation's start time to its approximate midpoint (by adding an integer number of pulse periods) and then adding a phase offset determined by fitting the observed profile to a high signal-to-noise ratio "standard profile" for the same pulsar. For computational convenience this procedure was carried out in the Fourier transform domain (Taylor 1992). The TEMPO software package (Taylor & Weisberg 1989) was then used to transform the topocentric TOAs to the solar system barycenter, compute differences between observed TOAs and those derived from a model of pulsar spin-down behavior, and vary the model parameters so as to minimize the residuals in a least-squares sense. For pulsars with poorly determined initial parameters this procedure was iterated, perhaps including some trial-and-error in the initial parameter values (see Taylor 1989), until all pulse numbering ambiguities were resolved and the solution had converged.

3. TIMING PARAMETERS

Table 1 lists the best-fitting parameters from the TOA analysis of each pulsar, accompanied by three quantities characterizing its timing accuracy and rotational stability. The positions, periods P, and period derivatives $\dot{P}$ are quoted for an epoch near the midpoint of the data span, generally close to the middle of 1991. Coordinates are based on the J2000 reference frame of the DE200 solar system ephemeris (Standish 1982). Pulsars with previously unmeasured $\dot{P}$ are marked with an asterisk. The quoted parameter uncertainties are generally twice the formal standard deviations from a least-squares fit to the available TOAs. They are believed to be realistic 1 σ estimates of the combined random and systematic errors.

Over data spans of a few years or longer, many pulsars exhibit significant deviations from strictly deterministic spin-down behavior. The presence of such "timing noise" implies that the observed spin-down parameters are nonstationary; as a consequence, independent measurements of period derivative carried out several years apart can be expected to differ by more than the combined measurement uncertainties. Thirty-five pulsars in our data set were found to have timing noise as evidenced by postfit timing residuals significantly larger than the measurement uncertainties. In nearly all of these cases the most recognizable signature of excess noise was a low-frequency, quasi-cubic trend in the residuals. For these pulsars we used the following procedure to minimize parameter bias caused by timing noise. Higher order frequency derivatives $d^2\nu/dt^2$ ($\equiv\ddot{\nu}$), $d^3\nu/dt^3$, ..., where $\nu = 1/P$, were introduced as free parameters to absorb the unmodeled noise and thereby "whiten" the data. In some cases as many as five or six derivatives were required to remove unmodeled long-term trends.

The celestial coordinates and uncertainties obtained from such a solution were adopted as the best unbiased estimates, and their values appear in Table 1. With the coordinates held fixed and all higher order derivatives set to zero, the pulsar period and its first derivative were then determined, providing values that represent our best estimate of deterministic spin-down behavior averaged over the span of the observations.

For each pulsar we also carried out a solution with exactly one extra spin-down derivative. Its measured value $\ddot{\nu}$ and formal uncertainty $\sigma_{\ddot{\nu}}$ were used to compute a stability estimate Δ characterizing the pulsar clock error caused by stochastic timing noise. The phenomenological spin-down derivatives are defined by a Taylor series equated to the observed rotational phase,

$$\phi = \phi_0 + \nu t + \tfrac{1}{2}\dot{\nu}t^2 + \tfrac{1}{6}\ddot{\nu}t^3 \ldots , \quad (1)$$

where ϕ_0 is the phase (in cycles) at time $t = 0$. The fourth term in equation (1), which is fixed at zero in the default timing model, can be used to estimate the cumulative phase contributed by timing noise over time interval t. We arbitrarily adopt a reference time interval of $t = 10^8$ s, close to the length of our data span, and define our stability parameter as

$$\Delta(t) = \log\left(\frac{1}{6\nu}\,|\ddot{\nu}|\,t^3\right), \quad (2)$$

if $|\ddot{\nu}| > 2\sigma_{\ddot{\nu}}$; otherwise, we quote an upper limit $\Delta(t) < \log(2\sigma_{\ddot{\nu}}t^3/6\nu)$. Table 1 lists values of $\Delta_8 \equiv \Delta(10^8\ \mathrm{s})$ for each pulsar, in addition to the post-fit rms residuals for the whitened timing solution (labeled σ_W) and for the deterministic solution containing only one timing derivative (labeled σ_R for red noise). For pulsars with timing noise at a level below our timing precision, σ_W is nearly identical to σ_R, as expected.

We note that our parameter Δ_8 is closely related to the activity parameter A defined by Cordes & Helfand (1980): A is the logarithm of the ratio of residual phase of a pulsar (after removal of white noise) to that measured in the Crab pulsar over the same time span. For a uniformly, continuously sampled pulsar with no measurement noise and a dominant cubic residual, the parameters are related by $A = \Delta_8 + 0.42$ for timing measurements spanning 10^8 s. We prefer the definition of Δ to that of A for several reasons. It is defined in an absolute sense rather than relative to another stochastic quantity (the timing noise in the Crab pulsar), and its numerical value is informative, being the base-10 logarithm of the pulsar clock error, in seconds, over the reference time interval.

Figure 1 illustrates the dependence of the timing noise parameter Δ_8 on period derivative. In addition to the 96 pulsars whose timing parameters appear in Table 1, we have computed Δ_8 for a number of others, including several millisecond/recycled pulsars (we used the data set of Dewey et al. 1988, among others). It should be emphasized that Δ measures a stochastic noise process, and is itself a random variable; it is thus fully expected that estimates of Δ from non-overlapping data sets will not be identical. Our results confirm and greatly strengthen the correlation between pulsar timing noise and spin-down rate first noted by Cordes & Downs (1985). The sloping line in Figure 1 corresponds to the relation

$$\Delta_8 = 6.6 + 0.6 \log \dot{P}\,, \quad (3)$$

which was fitted to the data by eye and which appears to characterize the timing noise of most pulsars fairly well, although there is a large scatter in the data. It should be noted

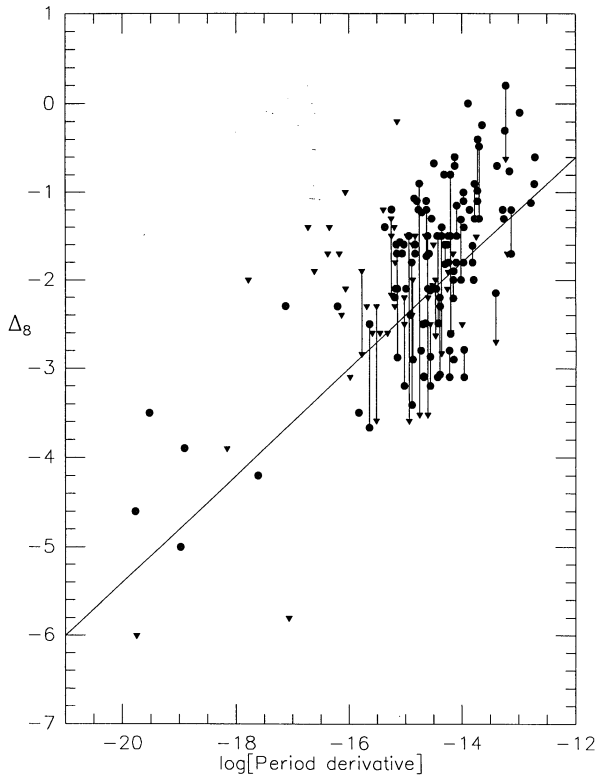

FIG. 1.—The timing noise parameter, Δ_8, plotted as a function of period derivative for 139 pulsars. Inverted triangles represent upper limits. When two or more estimates of Δ_8 are available, the corresponding plotted points are connected by vertical lines.

that the true relation may be somewhat steeper because the Δ_8 values measured for some of the pulsars with the smallest period derivatives may be measuring noise related to, e.g., the solar system ephemeris, the interstellar medium, or the reference atomic clocks, rather than intrinsic pulsar noise (Stinebring et al. 1990). A more extensive statistical analysis of the stability parameters of a larger set of pulsars is underway.

In addition to stochastic timing noise, some pulsars (especially young ones) also exhibit occasional, unpredictable "glitches" in their spin behavior: sudden spin-up followed by slow relaxation to roughly their original (extrapolated) periods. We observed only one glitch in our 3.7 yr data set of 96 pulsars: the PSR B1800−21 TOAs showed a glitch near the end of 1990 December (Lyne 1992). Our preglitch data for this pulsar consist of just one session in 1990 October; the first postglitch observations were in 1991 February. The postglitch pulse phase is well-characterized by a single exponential decay added to the first three terms of equation (1), yielding

$$\phi = \phi_0 + \nu t + \tfrac{1}{2}\dot{\nu}t^2 + ae^{-(t-t_0)/\tau}\,. \quad (4)$$

Our measurements are consistent with a timescale $\tau = 259 \pm 6$ days and an amplitude at our first postglitch observation (on MJD 48294.56, chosen as t_0) of $a = 14.6 \pm 0.5$ rotational periods. The spin-down parameters of PSR B1800−21 quoted in Table 1 were calculated after compensating for this exponential term. Without knowing the precise time of the glitch, it is impossible to calculate the instantaneous frequency change. We estimate, however, the long-term effect of the glitch by extrapolating the postglitch P and $\dot{P}$ back to our 1990 October observations and comparing the extrapolated and measured

1994ApJ...422..671A

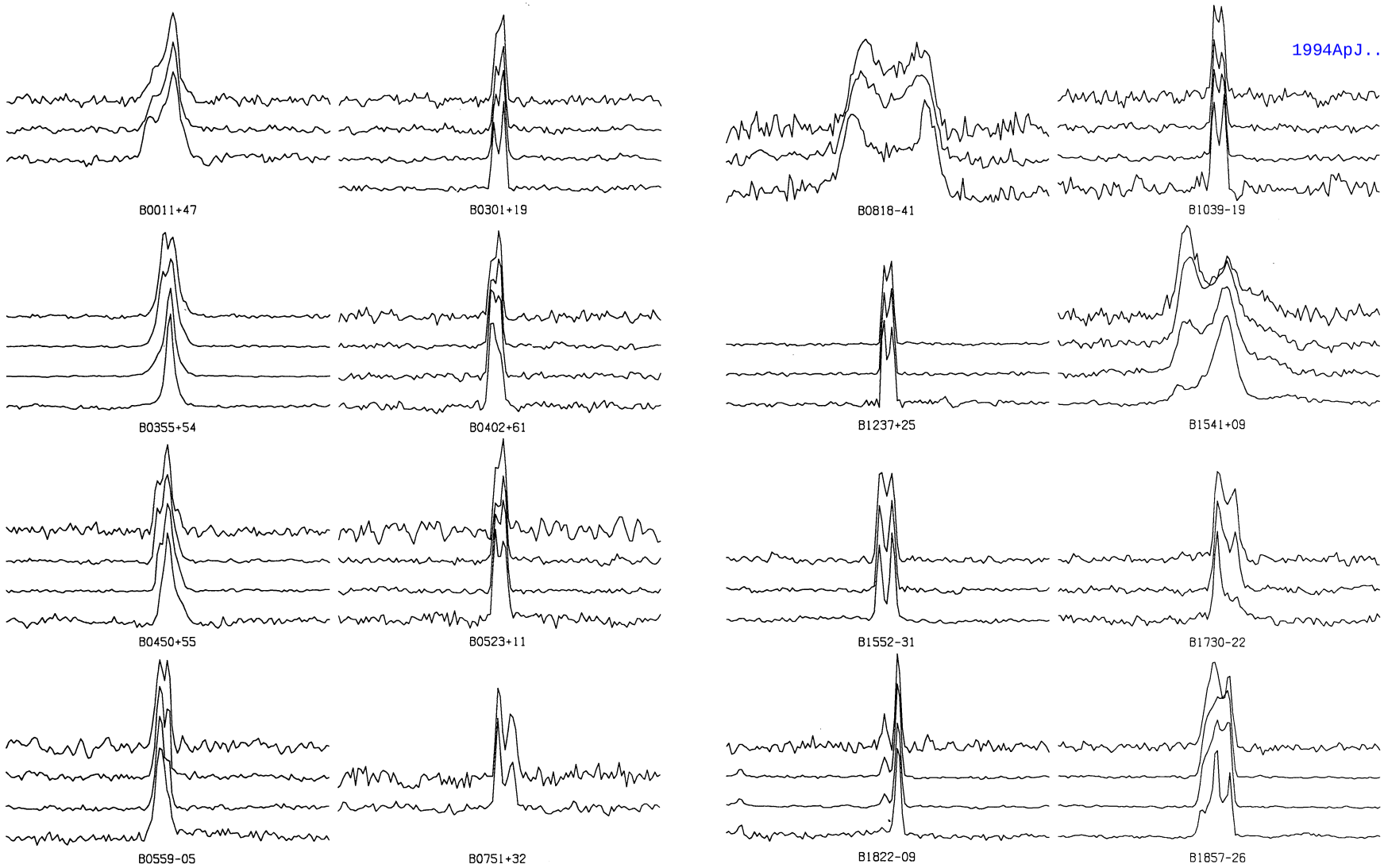

FIG. 2.—Pulse shapes of 24 pulsars that show significant changes over the frequency range 0.4–1.64 GHz. Full pulse periods are displayed with a resolution of 128 phase bins. Profiles in each group are plotted upward in order of increasing frequency: 0.4, 0.8, 1.33, and 1.64 GHz, with gaps indicating unavailable data.

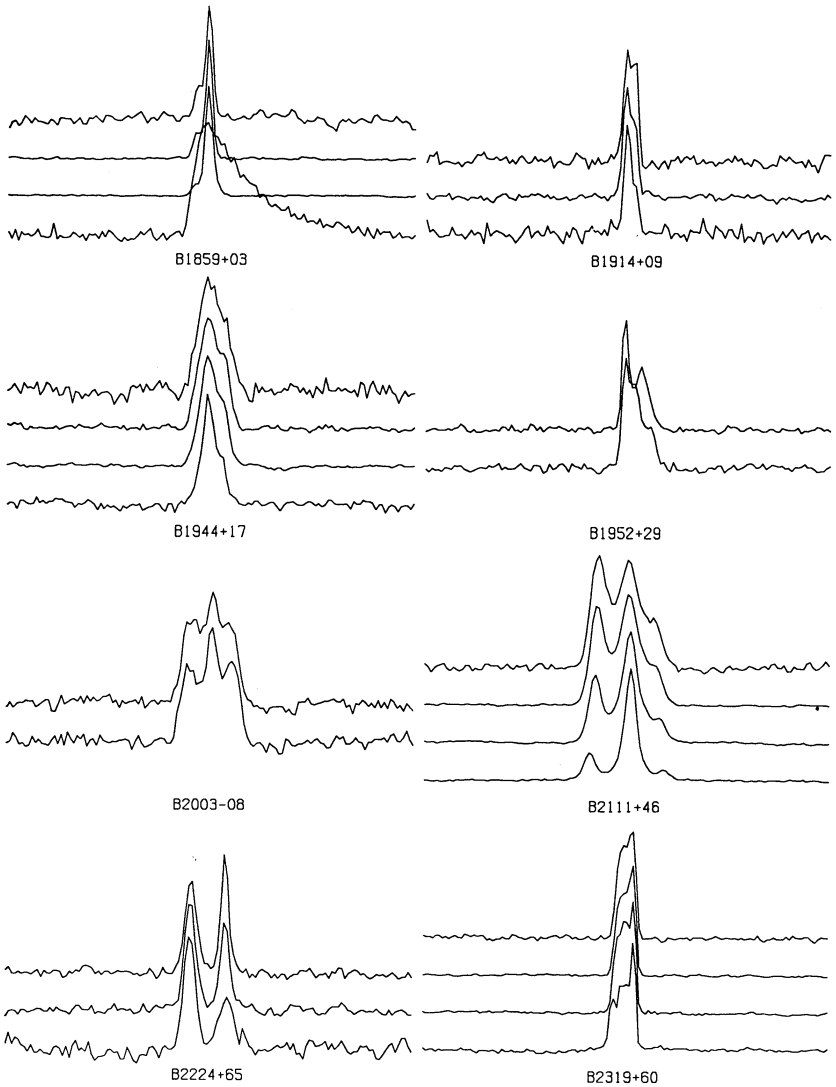

FIG. 2—*Continued*

pulse periods. This calculation yields

$$\frac{\Delta v}{v} = -\frac{\Delta P}{P} = 4 \times 10^{-6} . \quad (5)$$

Finally, timing observations at widely separated frequencies allow accurate measurements of pulsar dispersion measures. Intrinsic changes of pulse shape with frequency, however, can complicate the process by introducing frequency-dependent offsets in the TOAs which can be misinterpreted as incremental dispersion. The modest time resolution of our profiles (only 128 samples per period) made it impractical to try to identify a common "fiducial point" on the pulse profile and to track that point at each observing frequency with an accuracy comparable to σ_W (as done, for example, by Phillips & Wolszczan 1992). Instead, when frequency-dependent offsets were clearly present, we obtained a dispersion measurement using only data from single channels of the 20 or 40 MHz passband at 0.4 or 0.8 GHz.

4. PULSE SHAPES

Figures 2 and 3 display the pulse profiles of 96 pulsars timed regularly in this project, and eight others observed occasionally with the same system. Twenty-four pulsars yielding high signal-to-noise ratios at two or more observing frequencies and showing evidence of shape changes with frequency are illustrated in Figure 2. For each pulsar, four stacked profiles represent data acquired at 0.4, 0.8, 1.33, and 1.64 GHz, from bottom to top; blank spaces are left for any missing frequencies. In all cases the full period is plotted. Most of the previously known trends of pulse shape evolution with frequency are represented here: for example, PSRs B0355+54, B0450+55, B1541+09, B1822−09, B1857−26, and B2111+46 have "core" emission components which dominate at the lowest frequencies, while "cone" components become relatively prominent above 1 GHz (Rankin 1983; Lyne & Manchester 1988). On the other hand, PSR B0011+47 seems to go against this trend with a relatively prominent leading

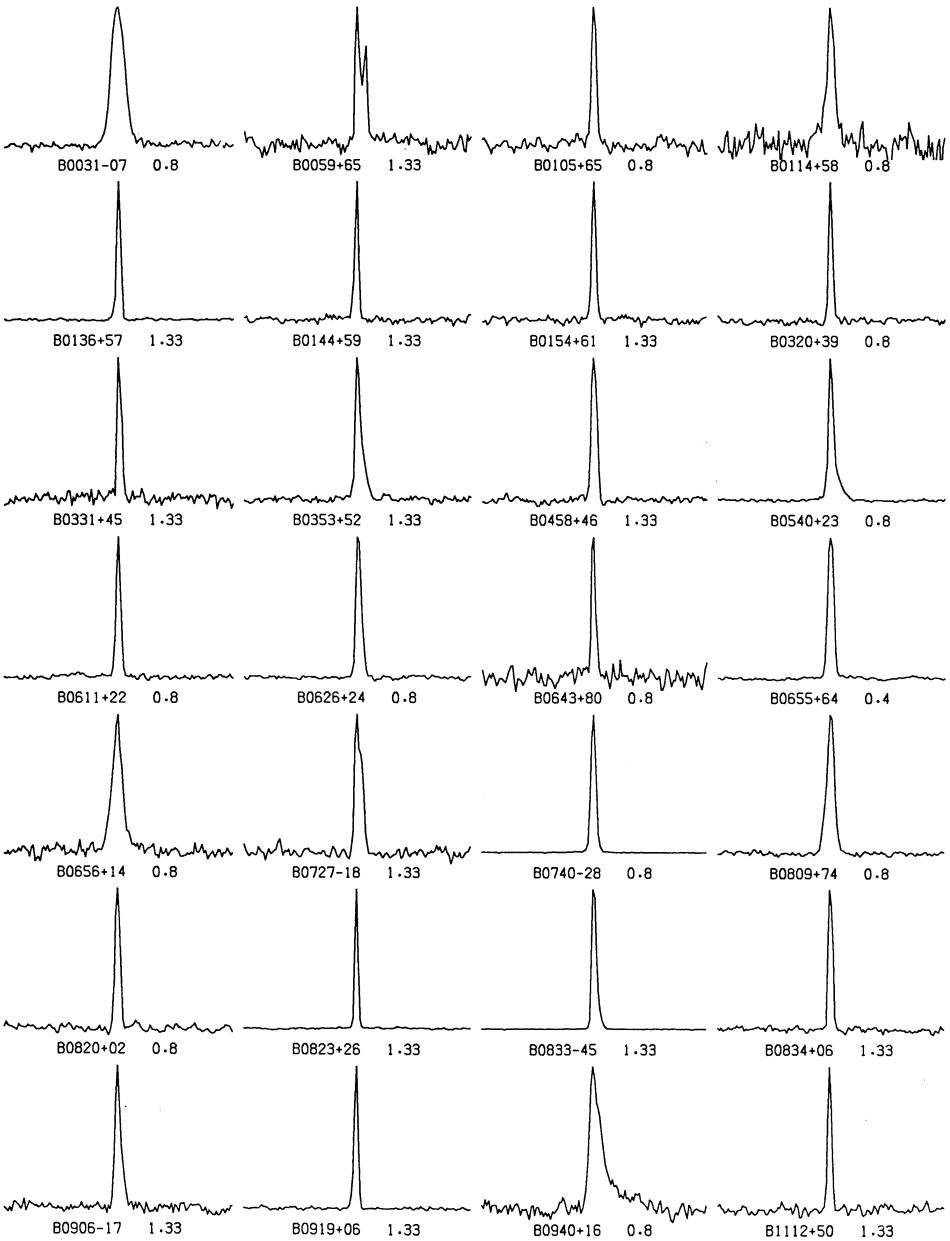

FIG. 3.—Observed pulse shapes of 80 pulsars. Full pulse periods are displayed with a resolution of 128 phase bins, and observing frequencies are given in GHz. For completeness we have included plots of a handful of pulsars whose timing models do not appear in Table 1. PSRs B0833−45, B1737−30, and B1933+16 were not primary targets of our timing program; the timing properties of PSRs B0655+64, B0820+02, B1620−26, B1744−24, and B1820−11 have been (or will be) published elsewhere.

component at 0.8 GHz that fades away at higher frequencies. Most profiles with clearly resolved multiple components are seen to spread slightly at the lower frequencies, again in accord with previously noted trends (Thorsett 1991 and references therein). PSR B1859+03, the most highly dispersed pulsar on our observing list, shows a pronounced scattering tail at 0.42 GHz, well modeled by a single-sided exponential of width 76 ± 7 ms (in good agreement with a measurement made by Rankin & Benson 1981). Such tails are known to scale with frequency approximately as $f^{-4.4}$ (Cordes, Weisberg, & Boriakoff 1985 and references therein), so it is not surprising that the effect is not visible in the three higher frequency profiles for this pulsar.

For the 80 remaining pulsars (Fig. 3), our observations show no strong evidence for changes of pulse shape with frequency. Many of the measured profiles are barely resolved in our data, with half-intensity widths no larger than three to six bins of the 128 bin period. Clear "interpulses" about half a period away from the main peak are visible in the profiles of PSRs B1702−19, B1822−09 (Fig. 2), B1929+10, and B2022+50. The first three of these have been reported previously, but the interpulse for PSR B2022+50 was not known before. It has a separation of $(180 \pm 3)^\circ$ from the main peak and a relative intensity of (0.22 ± 0.04) at 1.33 GHz. Three other pulsars we have observed, PSRs B0823+26, B1719−37, and B1944+17, are known to have weak interpulses (Taylor, Manchester, &

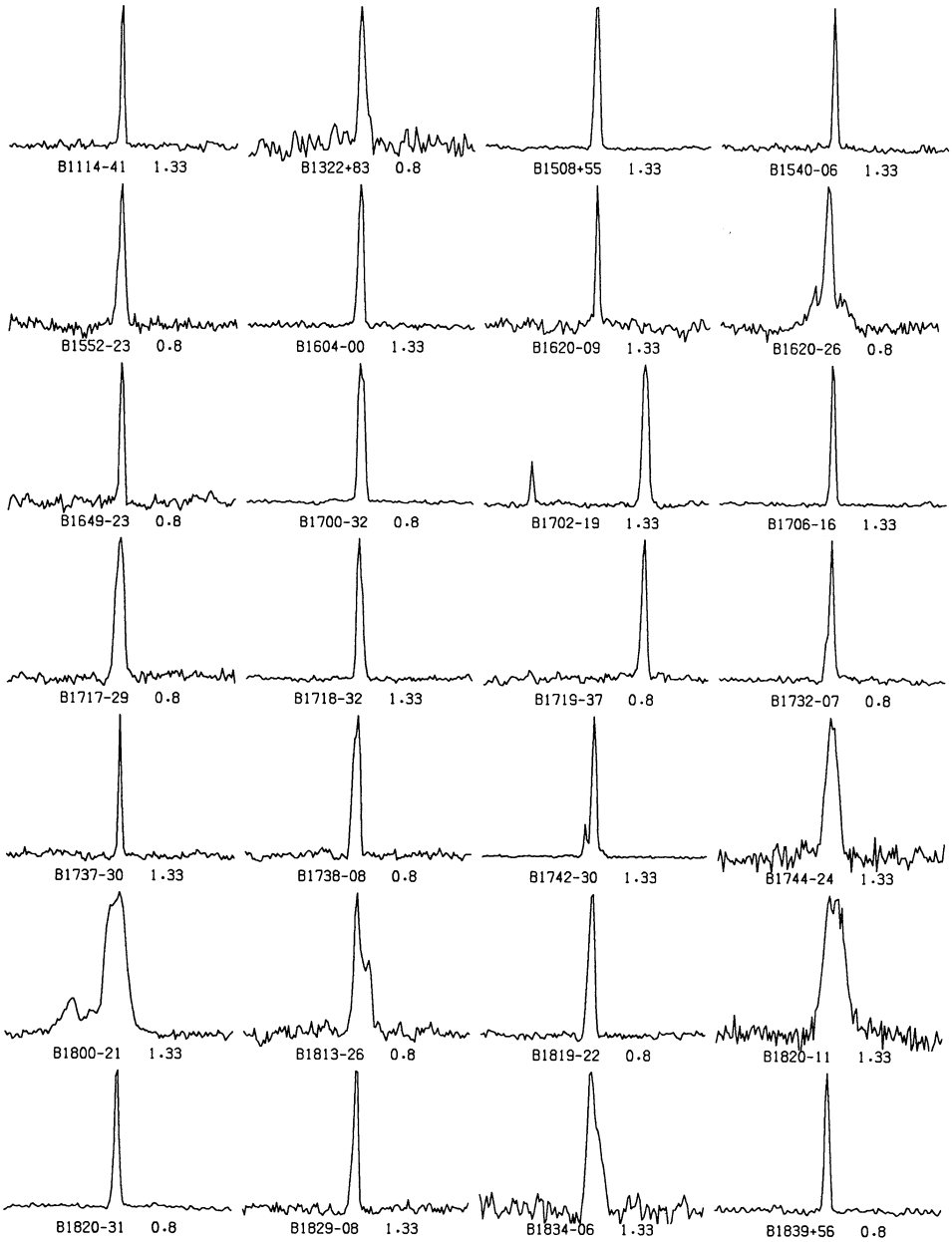

FIG. 3—*Continued*

Lyne 1993), but we cannot unambiguously detect them above the noise levels in our template profiles.

Approximate pulse widths, w_{10} and w_{50}, measured at 10% and 50% of the peak intensity, are listed in Table 2 for all pulsar-frequency combinations yielding good signal-to-noise ratios. The widths are quoted in milliperiods, and were measured using a simple straight-line interpolation between the binned intensities. Some profiles showed baseline noise of order 10% of the peak height; for these sources we list only the 50% widths. The uncertainties in the quoted widths are about one phase bin, i.e., 8 milliperiods.

5. DISCUSSION AND COMPARISON WITH PREVIOUS WORK

Many of the parameters listed in Tables 1 and 2 have been measured before. With a few notable exceptions, our results are in accord with existing measurements, and they usually improve somewhat on previously available accuracies. We have identified a systematic error apparently affecting all of the dispersion measures reported by Dewey et al. (1988). Fifteen pulsars were common to their list and ours, and we find their quoted values of DM to be systematically low by approximately 2% compared with our own. On the other hand, we find good agreement between DMs measured for 43 pulsars and those also determined by Hamilton & Lyne (1988). We suspect that the slightly biased values quoted by Dewey et al. (1988) are related to operational details of the hardware dedisperser they used.

Our value for the dispersion measure of PSR B1930+22 is 219.05 ± 0.04 cm^{-3} pc, more than 10 standard deviations above the value 211.3 ± 0.6 cm^{-3} pc quoted by Hankins

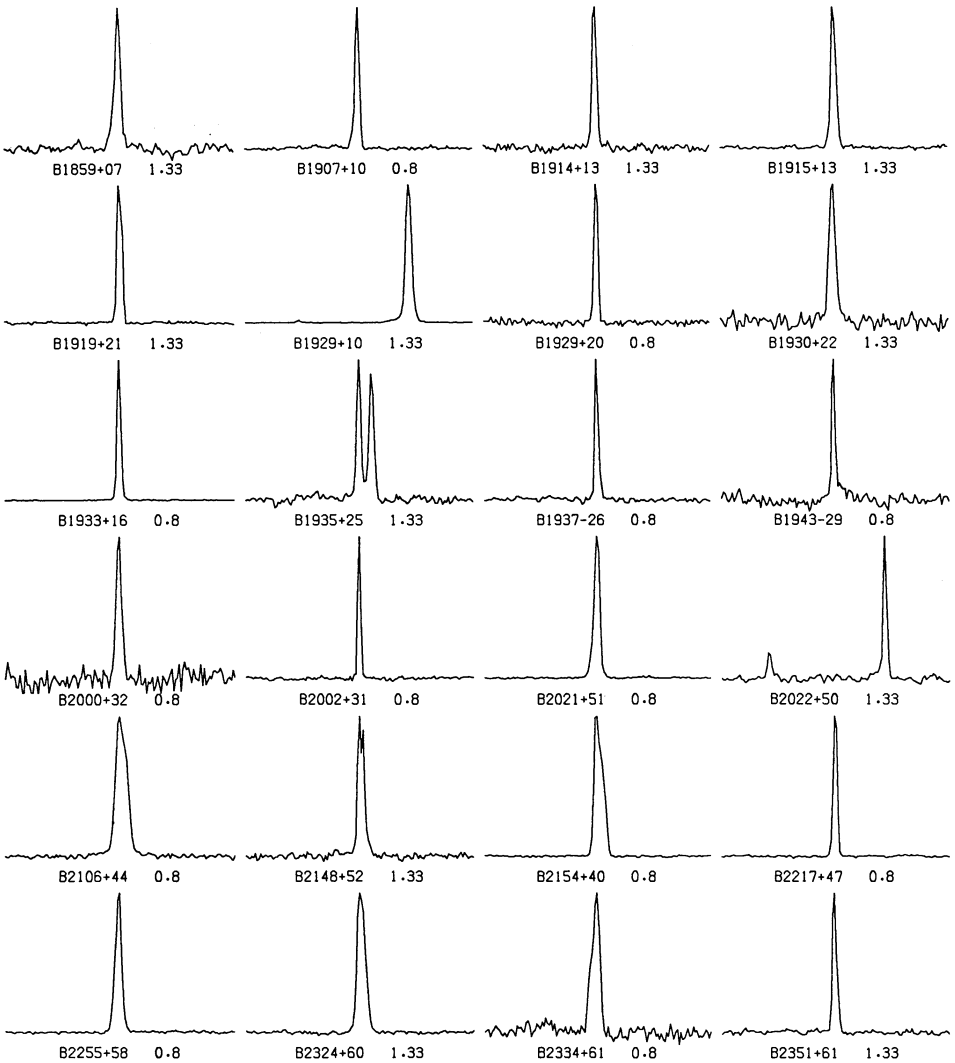

FIG. 3—*Continued*

(1987). To verify our own measurement, we timed a subset of data collected at various frequencies in the range 685–815 MHz and found DM = 218.5 ± 1.0 cm^{-3} pc. We note, in addition, that our tabulated DM is consistent with the value quoted in the discovery paper for this pulsar, namely = 219 ± 5 cm^{-3} pc (Hulse & Taylor 1975).

The celestial coordinates of PSR B1700−32 have been significantly improved, revealing a 14′ error in its declination as measured by Vivekanand, Mohanty, & Salter (1983). Most of our measurements were made while pointing at the incorrect position; however, the error is less than the half-power beam width of the 43 m telescope at 1.33 GHz. An error of 14′ is much too large to be caused by timing noise of plausible magnitude, and our observations show in any case that the rotational behavior of this pulsar is very stable, with $\Delta_8 < -1.8$. We believe that the earlier position measurement must be in error.

Finally, we believe that previously published timing solutions for PSRs B1935+25 (Dewey et al. 1988) and B2324+60 (Backus, Taylor, & Damashek 1982) are incorrect, probably as a result of pulse-numbering errors across gaps in the observations. Our tabulated solutions have successfully predicted the pulse periods and phases for these pulsars over the last few observing sessions which strongly suggests that our solutions are valid. For PSR B1935+25 we have, in addition, successfully fit to our model the TOAs obtained by Dewey et al. (1988). We have not been able to unambiguously phase-connect the earlier PSR B2324+60 data from Backus, Taylor, & Damashek (1982) with our own, but we find that both data sets are fully consistent with our solution.

R. Dewey and D. R. Stinebring made contributions to the early stages of this project. We thank the staff of NRAO Green Bank for their cooperation and valuable assistance. The NRAO is operated by Associated Universities, Inc., under cooperative agreement with the National Science Foundation. This work was supported by grants from NASA and the NSF.

TABLE 2

PULSE WIDTHS IN MILLIPERIODS[a]

PSR	f (GHz)	w_{10} (mP)	w_{50} (mP)	PSR	f (GHz)	w_{10} (mP)	w_{50} (mP)	PSR	f (GHz)	w_{10} (mP)	w_{50} (mP)
B0011+47	0.8	153	91	B0833−45	1.33	50	24	B1834−06	1.33		58
B0011+47	1.33	138	49	B0834+06	1.33	38	25	B1839+56	0.8	43	24
B0011+47	1.64		42	B0906−17	1.33	62	27	B1857−26	0.4	116	62
B0031−07	0.8	120	69	B0919+06	1.33	39	19	B1857−26	0.8	116	90
B0059+65	1.33	70	53	B0940+16	0.8		62	B1857−26	1.33	114	89
B0105+65	0.8	46	25	B1039−19	0.4		50	B1857−26	1.64	117	84
B0114+58	0.8		36	B1039−19	0.8	60	45	B1859+03	0.4		131
B0136+57	1.33	41	21	B1039−19	1.33	60	43	B1859+03	0.8	59	23
B0144+59	1.33	40	17	B1039−19	1.64		42	B1859+03	1.33	61	20
B0154+61	1.33	43	21	B1112+50	1.33	38	21	B1859+03	1.64		22
B0301+19	0.4	58	44	B1114−41	1.33	35	18	B1859+07	1.33	70	28
B0301+19	0.8	59	40	B1237+25	0.4	52	43	B1907+10	0.8	47	22
B0301+19	1.33	52	35	B1237+25	0.8	52	39	B1914+09	0.4		24
B0301+19	1.64	52	36	B1237+25	1.33	51	37	B1914+09	0.8	59	38
B0320+39	0.8	38	20	B1322+83	0.8		32	B1914+09	1.33	58	39
B0331+45	1.33	41	24	B1508+55	1.33	46	28	B1914+13	1.33	44	24
B0353+52	1.33	73	27	B1540−06	1.33	36	18	B1915+13	1.33	52	26
B0355+54	0.4	73	29	B1541+09	0.4	236	76	B1919+21	1.33	45	28
B0355+54	0.8	104	32	B1541+09	0.8		184	B1929+10	1.33	59	31
B0355+54	1.33	113	57	B1541+09	1.33	338	191	B1929+20	0.8	38	21
B0355+54	1.64	111	57	B1541+09	1.64		184	B1930+22	1.33	62	34
B0402+61	0.4	63	42	B1552−23	0.8	61	29	B1933+16	0.8	38	20
B0402+61	0.8	60	43	B1552−31	0.4	76	58	B1935+25	1.33	100	77
B0402+61	1.33	58	40	B1552−31	0.8	72	57	B1937−26	0.8	39	17
B0402+61	1.64		41	B1552−31	1.33	73	57	B1943−29	0.8		18
B0450+55	0.4	87	35	B1552−31	1.64		55	B1944+17	0.4	92	37
B0450+55	0.8	89	47	B1604−00	1.33	49	27	B1944+17	0.8	110	66
B0450+55	1.33	88	53	B1620−09	1.33	36	17	B1944+17	1.33	116	78
B0450+55	1.64		50	B1620−26	1.33		34	B1944+17	1.64		72
B0458+46	1.33	51	31	B1649−23	0.8	38	22	B1952+29	1.33	95	57
B0523+11	0.4		47	B1700−32	0.8	54	36	B2000+32	0.8		28
B0523+11	0.8	59	44	B1702−19	1.33		33	B2002+31	0.8	28	15
B0523+11	1.33	59	41	B1706−16	1.33	40	20	B2003−08	1.33	173	133
B0523+11	1.64		39	B1717−29	0.8	68	44	B2021+51	0.8	57	29
B0540+23	0.8	74	26	B1718−32	1.33	50	30	B2022+50	1.33		18
B0559−05	0.4	84	42	B1719−37	0.8	52	26	B2106+44	0.8	97	60
B0559−05	0.8	69	44	B1730−22	0.4	110	23	B2111+46	0.4		35
B0559−05	1.33	67	46	B1730−22	0.8	104	74	B2111+46	0.8	208	118
B0559−05	1.64		50	B1730−22	1.33	107	76	B2111+46	1.33	207	131
B0611+22	0.8	45	23	B1732−07	0.8	56	22	B2111+46	1.64	208	133
B0626+24	0.8	52	28	B1737−30	1.33	29	13	B2148+52	1.33	62	34
B0643+80	0.8		20	B1738−08	0.8	56	38	B2154+40	0.8	77	48
B0655+64	0.4	54	32	B1742−30	1.33		24	B2217+47	0.8	38	20
B0656+14	0.8	110	48	B1800−21	1.33		103	B2224+65	0.4		34
B0727−18	1.33	62	40	B1813−26	0.8	108	71	B2224+65	0.8		112
B0740−28	0.8	49	29	B1819−22	0.8	55	33	B2224+65	1.33		107
B0751+32	0.8	75	54	B1820−11	1.33		105	B2255+58	0.8	62	32
B0809+74	1.33	80	45	B1820−31	0.8	47	23	B2319+60	1.33	69	51
B0818−41	0.4		291	B1822−09	0.4		19	B2324+60	1.33	74	42
B0818−41	0.8		278	B1822−09	0.8		20	B2334+61	0.8		43
B0818−41	1.33		260	B1822−09	1.33		20	B2351+61	1.33	43	22
B0820+02	0.8	45	26	B1822−09	1.64		20				
B0823+26	1.33	30	15	B1829−08	1.33	50	23				

[a] Calculated from profiles displayed in Figs. 2 and 3. The measurement uncertainty is ~8 mP for all values.

REFERENCES

Backus, P. R., Taylor, J. H., & Damashek, M. 1982, ApJ, 255, L63
Cordes, J. M., & Downs, G. S. 1985, ApJS, 59, 343
Cordes, J. M., & Helfand, D. J. 1980, ApJ, 239, 640
Cordes, J. M., Weisberg, J. M., & Boriakoff, V. 1985, ApJ, 288, 221
Dewey, R. J., Taylor, J. H., Maguire, C. M., & Stokes, G. H. 1988, ApJ, 332, 762
Downs, G. S., & Reichley, P. E. 1983, ApJS, 53, 169
Hamilton, P. A., & Lyne, A. G. 1988, MNRAS, 224, 1073
Hankins, T. H. 1987, ApJ, 312, 276
Hulse, R. A., & Taylor, J. H. 1975, ApJ, 201, L55
Lyne, A. G. 1992, Phil. Trans. Roy. Soc. London A, 341, 29
Lyne, A. G., & Manchester, R. N. 1988, MNRAS, 234, 477
Phillips, J. A., & Wolszczan, A. 1992, ApJ, 385, 273
Rankin, J. M. 1983, ApJ, 274, 333
Rankin, J. M., & Benson, J. M. 1981, AJ, 86, 418
Standish, E. M. 1982, A&A, 114, 297
Stinebring, D. R., Ryba, M. F., Taylor, J. H., & Romani, R. W. 1990, Phys. Rev. Lett., 65, 285
Taylor, J. H. 1989, in Timing Neutron Stars ed. H. Ögelman & E. P. J. van den Heuvel (Dordrecht: Kluwer), 17
———. 1992, Phil. Trans. Roy. Soc. A, 341, 117
Taylor, J. H., Manchester, R. N., & Lyne, A. G. 1993, ApJS, 88, 529
Taylor, J. H., & Weisberg, J. M. 1989, ApJ, 345, 434
Thorsett, S. E. 1991, ApJ, 377, 263
Vivekanand, M., Mohanty, D. K., & Salter, C. J. 1983, MNRAS, 204, 81P